Multilayer primitive equations model with velocity shear and stratification

By F. J. BERON-VERA
Rosenstiel School of Marine and Atmospheric Science, University of Miami,
4600 Rickenbacker Cswy., Miami, FL 33149, USA
fberon@rsmas.miami.edu

(Received 11 December 2003)

The purpose of this paper is to present a multilayer primitive equations model for ocean dynamics in which the velocity and buoyancy fields within each layer are not only allowed to vary arbitrarily with horizontal position and time, but also with depth—linearly at most. The model is a generalization of Ripa's inhomogeneous one-layer model to an arbitrary number of layers. Unlike models with homogeneous layers, the present model is able to represent thermodynamics processes. Unlike models with slab layers, i.e. those in which the layer velocity and buoyancy fields are depth-independent, the present model can represent explicitly the thermal-wind balance within each layer which dominates at low frequency. In the absence of external forcing and dissipation, energy, volume, mass, and buoyancy variance constrain the dynamics; conservation of total zonal momentum requires in addition the usual zonal symmetry of the topography and horizontal domain. The model further possesses a singular Hamiltonian structure. Unlike the single-layer counterpart, however, no steady solution has been possible to prove formally (or Arnold) stable using the above invariants. It is shown here that a model with only two layers provides an excellent representation of the exact gravest baroclinic mode phase speed. This suggests that configurations with only a small number of layers will be needed to tackle a large variety of problems with enough realism.

1. Introduction

Approximate inhomogeneous layer primitive equations models in which the velocity and buoyancy fields are allowed to vary only in the horizontal position and time (Dronkers 1969; Lavoie 1972) have been very extensively exploited in ocean modeling. For instance, a model with only one "slab" active layer (i.e. floating on top of a denser homogeneous quiescent infinitely deep layer) has been shown useful to study processes near the ocean surface which, in addition to wind drag, is subject to nonuniform heat and freshwater fluxes (e.g. Young 1994; Young & Chen 1995; Fukamachi *et al.* 1995; Ripa 1996; Røed 1997; Scott & Willmott 2002). The main motivation for the use of these type of models is the observation that in the upper part of the ocean a vertically well-mixed layer separated from the underlying heavier fluid by a well-defined pycnocline often develops. Also, the slab models are numerically very efficient, particularly in the study of meso- and submesoscale ocean dynamics as they can resolve, for a given computational cost, finer horizontal scales than fully three-dimensional models (Eldevik 2002). However, applications are not restricted to the study upper-ocean processes only. In these applications, a stack of homogeneous and inhomogeneous active layers is usually considered; Ripa (1993) has derived a model with an arbitrary number of active slab layers. Examples of these applications include one-dimensional (in the horizontal) modeling efforts, typically oriented to provide insight into the basic physics underlying the heat and salt balances in semienclosed seas (e.g. Ripa 1997; Beron-Vera & Ripa 2002; Ripa 2001); and two-dimensional regional ocean modeling efforts (e.g. Szoeke & Richman 1984; Anderson & McCreary 1985*b*; McCreary & Kundu 1988; McCreary *et al.* 1989, 1991, 1993, 1996*a*; Beier 1997; Beier & Ripa 1999; Røed & Shi 1999; Palacios-Hernández *et al.* 2002). Other applications include the study of biophysical interactions (e.g. McCreary *et al.* 1996*b*, 2001; Hood *et al.* 2003), equatorial dynamics (e.g. Anderson & McCreary 1985*a*; McCreary & Yu 1992), and ENSO predictability (e.g. Schopf & Cane 1983; Balmaseda *et al.* 1994). Furthermore, in the widely used Miami Isopycnic-Coordinate Ocean Model (MICOM) the upper layer is chosen to be a slab-like layer (Bleck *et al.* 1992).

Despite their widespread use, the slab models are known to have several limitations and deficiencies Ripa (1999): (*a*) they cannot represent explicitly the thermal-wind balance which dominates at low frequencies; and (*b*) they have a zero-frequency mode in which the layer thickness and buoyancy changes without changing the flow, and whose unlimited growth cannot be prevented by the invariants that constrain the (inviscid unforced) system. Eldevik (2002) has recently pointed out also that the slab models cannot satisfactorily represent frontogenesis, a process for which the thermal-wind balance is fundamental.

To cure the slab model limitations and deficiencies, Ripa (1995, hereinafter referred to as R95) proposed an improved closure to partially incorporate thermodynamic processes in a one-layer model. In addition to allowing arbitrary velocity and buoyancy variations in horizontal position and time, Ripa's model allows the velocity and buoyancy fields to vary linearly with depth. Ripa's model enjoys a number of properties which make it very promising. For instance, (*a*) it represents explicitly the thermal-wind balance at low frequencies; and (*b*) with only one layer the free waves supported by the model (Poincaré, Rossby, midlatitude coastal Kelvin, equatorial, etc.) are a very good approximation to the first and second vertical modes in the fully three-dimensional model.

In this work I present a generalization of Ripa's model to an arbitrary number of layers, including two possible (mathematically equivalent) vertical configurations (§ 2). The goal is to generalize Ripa's model, allowing enough flexibility to treat more complicated problems than those that can be tackled with only one layer. Several aspects of the generalized model are discussed in §3. These include: its conservation laws; the Kelvin circulation theorems derived from the model; its Hamiltonian structure; the lack of formal stability theorems; results on vertical normal modes and remarks on baroclinic instability; and the incorporation of forcing in the model equations. Section 4 closes the paper with some concluding remarks.

2. The generalized model

Consider a stack of n active fluid layers with thickness $h_i(\mathbf{x}, t)$, $i = 1, \cdots, n$, where $\mathbf{x}$ is the horizontal position and t the time (figure 1). The geometry can be either planar or spherical; in the former case the vertical coordinate, z, is perpendicular to the plane, whereas in the latter it is radial. The total thickness is $h(\mathbf{x}, t) = \sum_j h_j(\mathbf{x}, t)$. The stack of inhomogeneous layers can be either limited from below by a rigid bottom, $z = h_0(\mathbf{x})$, or from above by a rigid lid, $z = -h_0(\mathbf{x})$. The usual choice in the rigid lid case is $h_0 \equiv 0$; however, laboratory experiments are often design to have a nonhorizontal top lid. The remaining boundary in the rigid-bottom (resp., rigid-lid) configuration is a soft interface with a passive infinitely thick layer of lighter (resp., denser) homogeneous fluid of density ρ_{n+1}. Although vacuum ($\rho_{n+1} \equiv 0$) is the typical setting in the rigid-bottom configuration, the choice $\rho_{n+1} \neq 0$ is useful in the study of deep flows over topography.

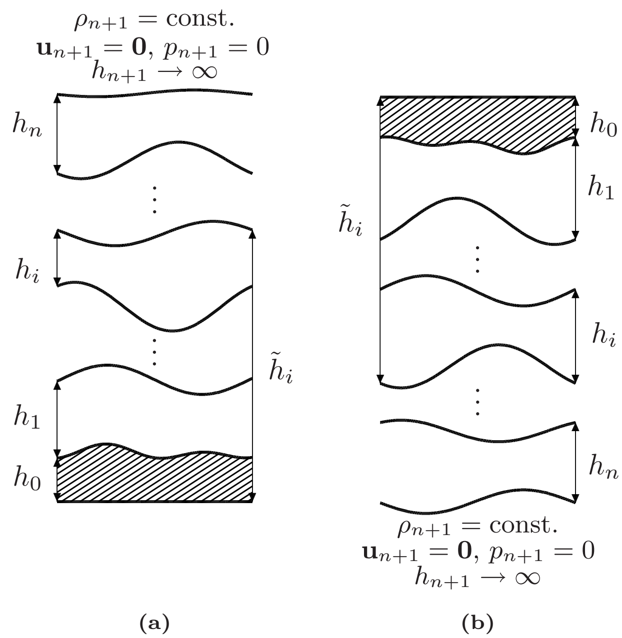

FIGURE 1. Sketch of the layered model. The two possible vertical configurations of the model are rigid bottom (a) and rigid lid (b). Within each layer the velocity and buoyancy fields not only vary arbitrarily with the horizontal position and time, but also linearly with depth.

Following R95 closely, I consider the ansatz

$$\mathbf{u}_i(\mathbf{x}, \sigma, t) = \bar{\mathbf{u}}_i(\mathbf{x}, t) + \sigma \mathbf{u}_i^\sigma(\mathbf{x}, t), \tag{2.1a}$$

$$\vartheta_i(\mathbf{x}, \sigma, t) = \bar{\vartheta}_i(\mathbf{x}, t) + \sigma \vartheta_i^\sigma(\mathbf{x}, t), \tag{2.1b}$$

for the ith-layer horizontal velocity and buoyancy fields. Here,

$$\bar{a}_i := \tfrac{1}{2} \int_{-1}^{+1} \mathrm{d}\sigma\, a, \tag{2.2}$$

which is the vertical average of any variable $a(\mathbf{x}, \sigma, t)$ within the ith layer. The ith-layer buoyancy is defined as

$$\vartheta_i(\mathbf{x}, \sigma, t) := \pm g \left[\rho_i(\mathbf{x}, \sigma, t) - \rho_{n+1}\right] / \rho_{\mathrm{r}}, \tag{2.3}$$

where the upper (resp., lower) sign corresponds to the rigid-bottom (resp., rigid-lid). Here, g is gravity, $\rho_i(\mathbf{x}, \sigma, t) = \bar{\rho}_i(\mathbf{x}, t) + \sigma \rho_i^\sigma(\mathbf{x}, t)$ is the (variable) density in the ith layer, and ρ_{r} denotes the (constant) reference density used in the Boussinesq approximation. A key element for the derivation of the n-layer version of Ripa's model is the definition of the rescaled vertical coordinate σ so as to vary linearly from ± 1, at the base, to ∓ 1, at the top, of the ith layer (figure 2):

$$\pm z =: \tilde{h}_{i-1}(\mathbf{x}, t) + \frac{1 - \sigma}{2} h_i(\mathbf{x}, t), \tag{2.4}$$

where

$$\tilde{h}_i(\mathbf{x}, t) := h_0(\mathbf{x}) + \sum_{j=1}^{i} h_j(\mathbf{x}, t). \tag{2.5}$$

[Henceforth an upper (resp., lower) sign will correspond to the rigid-bottom (resp., rigid-

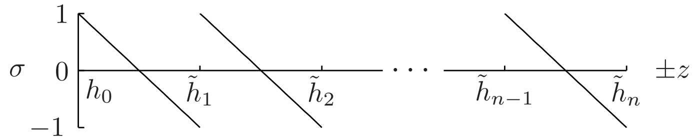

FIGURE 2. Vertical coordinate choice. Within each layer the rescaled vertical coordinate σ varies linearly from ±1, at the base, to ∓1, at the top. The upper (resp., lower) sign corresponds to the rigid-bottom (resp., rigid-lid) configuration of figure 1.

lid) configuration.] Physically admissible buoyancy values, i.e. everywhere positive and monotonically increasing (resp., decreasing) with depth in the rigid-bottom (resp., rig-lid) case, are such that

$$\bar\vartheta_i > \vartheta_i^\sigma > 0, \quad \bar\vartheta_i - \bar\vartheta_{i+1} \geqslant \vartheta_i^\sigma + \vartheta_{i+1}^\sigma. \tag{2.6}$$

Notice that $\vartheta_i^\sigma = \frac{1}{2}n_i^2 h_i$, where $n_i^2(\mathbf{x},t) > 0$ is the square of the instantaneous Brunt-Väisälä frequency within the ith layer.

In order to obtain the equations for the n-layer version of Ripa's model one must proceed as follows.

(a) Substitute the ansatz (2.1) in the (inviscid unforced) fully three-dimensional, i.e. exact, primitive equations defined in $h_0 < \pm z < h_0 + h$ with vertical velocity $w = \pm(\partial_t + \mathbf{u}\cdot\boldsymbol{\nabla})(h_0+h)$ at $z = \pm(h_0+h)$ and $w = \pm\mathbf{u}\cdot\boldsymbol{\nabla}h_0$ at $z = \pm h_0$, and kinematic pressure $p = 0$ at $z = \pm(h_0+h)$; here $\boldsymbol{\nabla}$ denotes the horizontal gradient.

(b) Replace all occurrences of σ^2 by its vertical average (i.e. $\sigma^2 \mapsto \frac{1}{3}$) to preserve the linear vertical structure within each layer.

(c) Collect terms in powers of σ and equate them to zero afterwards.

The resulting equations are:

$$\overline{\mathrm{D}_i\vartheta_i} = 0, \tag{2.7a}$$

$$(\mathrm{D}_i\vartheta_i)^\sigma = 0, \tag{2.7b}$$

$$\partial_t h_i + \boldsymbol{\nabla}\cdot h_i\bar{\mathbf{u}}_i = 0, \tag{2.7c}$$

$$\overline{\mathrm{D}_i\mathbf{u}_i} + f\hat{\mathbf{z}}\times\bar{\mathbf{u}}_i + \overline{\boldsymbol{\nabla}p}_i = \mathbf{0}, \tag{2.7d}$$

$$(\mathrm{D}_i\mathbf{u}_i)^\sigma + f\hat{\mathbf{z}}\times\mathbf{u}_i^\sigma + (\boldsymbol{\nabla}p_i)^\sigma = \mathbf{0}. \tag{2.7e}$$

Here, f is the Coriolis parameter; $\hat{\mathbf{z}}$ is the vertical unit vector;

$$\overline{\mathrm{D}_i\mathbf{a}} = (\partial_t + \bar{\mathbf{u}}_i\cdot\boldsymbol{\nabla})\bar{\mathbf{a}} + \tfrac{1}{3}h_i^{-1}\boldsymbol{\nabla}\cdot h_i\mathbf{u}_i^\sigma\mathbf{a}^\sigma, \tag{2.7f}$$

$$(\mathrm{D}_i\mathbf{a})^\sigma = (\partial_t + \bar{\mathbf{u}}_i\cdot\boldsymbol{\nabla})\mathbf{a}^\sigma + \mathbf{u}_i^\sigma\cdot\boldsymbol{\nabla}\bar{\mathbf{a}}, \tag{2.7g}$$

are the mean and σ components of the material derivative of any vector $\mathbf{a}(\mathbf{x},\sigma,t) = \bar{\mathbf{a}}(\mathbf{x},t) + \sigma\mathbf{a}^\sigma(\mathbf{x},t)$ in the ith layer; and

$$\overline{\boldsymbol{\nabla}p}_i = (\bar\vartheta_i - \tfrac{1}{3}\vartheta_i^\sigma)\boldsymbol{\nabla}h_i + \tfrac{1}{2}h_i\boldsymbol{\nabla}(\bar\vartheta_i - \tfrac{1}{3}\vartheta_i^\sigma) + \bar\vartheta_i\boldsymbol{\nabla}\tilde h_{i-1} + \boldsymbol{\nabla}\sum_{j=i+1}^{n} h_j\bar\vartheta_j, \tag{2.7h}$$

$$(\boldsymbol{\nabla}p_i)^\sigma = \tfrac{1}{2}\vartheta_i^\sigma\boldsymbol{\nabla}h_i + \tfrac{1}{2}h_i\boldsymbol{\nabla}\bar\vartheta_i + \vartheta_i^\sigma\boldsymbol{\nabla}\tilde h_{i-1}, \tag{2.7i}$$

which are the mean and σ components of the ith-layer pressure gradient force.

System (2.7) consists of $7n$ evolution equations in the $7n$ independent fields $(h_i, \bar\vartheta_i, \vartheta_i^\sigma, \bar{\mathbf{u}}_i, \mathbf{u}_i^\sigma, \cdots, h_n, \bar\vartheta_n, \vartheta_n^\sigma, \bar{\mathbf{u}}_n, \mathbf{u}_n^\sigma)$. The coupling among different layer quantities is provided by the last terms on the right hand side of the pressure forces (2.7h,i). It is important to notice that the dynamics in both the rigid-bottom and rigid-lid configurations is described by system (2.7); no double signs are necessary. The latter must be taken into account, however, in the computation of the total pressure in the ith layer, which, up to the addition of an irrelevant constant, is given by $\rho_{\rm r} p_i \pm \rho_{n+1} g z$, where

$$p_i = \tfrac{1}{2}\,(1+\sigma)\,h_i\bar{\vartheta}_i - \tfrac{1}{4}(1-\sigma^2)h_i\vartheta_i^\sigma + \sum_{j=i+1}^{n} h_j\bar{\vartheta}_j. \tag{2.7j}$$

The multilayer slab model follows from (2.7) upon neglecting $\mathbf{u}_i^\sigma$ and ϑ_i^σ. Ignoring $\mathbf{u}_i^\sigma$ in (2.7) results in a model with $\mathbf{u}_i^\sigma \equiv \mathbf{0}$ but $\vartheta_i^\sigma \neq 0$ which provides a generalization of Schopf & Cane's (1983) intermediate layer model. Alternatively, omission of ϑ_i^σ in system (2.7) gives a model with $\vartheta_i^\sigma \equiv 0$ but $\mathbf{u}_i^\sigma \neq \mathbf{0}$ that can be thought of, assuming a rigid-lid configuration, as the generalized multilayer nonsubinertial mixed-layer approximation of Young (1994). A initial state with uniform buoyancy inside each layer ($\bar{\vartheta}_i$ = const. and $\vartheta_i^\sigma \equiv 0$) and vanishing velocity vertical shear ($\mathbf{u}_i^\sigma \equiv \mathbf{0}$) is preserved by (2.7); as a consequence, unlike the above reduced models, the homogeneous layers model follows from (2.7) as a particular case, just as it does it from the fully three-dimensional model. It is important to notice that the homogeneous layers model is exact for a stepwise density stratification; however, it is not able to accommodate thermodynamic processes which are particularly important in the upper part of ocean.

3. Discussion of several aspects of the model

3.1. *Conservation laws*

In a closed domain, D, conservation of the ith-layer volume, mass, and buoyancy variance is enforced, respectively, because of (2.7c),

$$\partial_t(h_i\bar{\vartheta}_i) + \boldsymbol{\nabla}\cdot(h_i\bar{\vartheta}_i\bar{\mathbf{u}}_i + \tfrac{1}{3}\vartheta_i^\sigma\mathbf{u}_i^\sigma) = 0, \tag{3.1}$$

and

$$\partial_t\left(h_i\overline{\vartheta_i^2}\right) + \boldsymbol{\nabla}\cdot h_i\left(\overline{\vartheta_i^2}\bar{\mathbf{u}}_i + \tfrac{2}{3}\bar{\vartheta}_i\vartheta_i^\sigma\mathbf{u}_i^\sigma\right) = 0. \tag{3.2}$$

The total energy (sum of the energies in each layer) is also preserved in a closed domain as

$$\partial_t\sum_j E_j + \boldsymbol{\nabla}\cdot\sum_j h_j(\bar{b}_j\bar{\mathbf{u}}_j + \tfrac{1}{3}b_j^\sigma\mathbf{u}_j^\sigma) = 0, \tag{3.3a}$$

where

$$E_i := \tfrac{1}{2}h_i\bar{\mathbf{u}}_i^2 + \tfrac{1}{6}h_i(\mathbf{u}_i^\sigma)^2 + \tfrac{1}{2}h_i^2(\bar{\vartheta}_i - \tfrac{1}{3}\vartheta_i^\sigma) + h_i\tilde{h}_{i-1}\bar{\vartheta}_i, \tag{3.3b}$$

and

$$\bar{b}_i := \tfrac{1}{2}\bar{\mathbf{u}}_i^2 + \tfrac{1}{6}(\mathbf{u}_i^\sigma)^2 + h_i(\bar{\vartheta}_i - \tfrac{1}{3}\vartheta_i^\sigma) + \tilde{h}_{i-1}\bar{\vartheta}_i + \sum_{j=i+1}^{n} h_j\bar{\vartheta}_j, \tag{3.4a}$$

$$b_i^\sigma := \bar{\mathbf{u}}_i\cdot\mathbf{u}_i^\sigma + (\tilde{h}_{i-1} + \tfrac{1}{2}h_i)\vartheta_i^\sigma, \tag{3.4b}$$

which are the mean and σ components of the ith layer Bernoulli head. The above result follows upon realizing that $\sum_{j=1}^n h_j\bar{\vartheta}_j\partial_t\tilde{h}_{j-1} - \sum_{j=1}^n \partial_t h_j \sum_{k=j+1}^n h_k\bar{\vartheta}_k \equiv 0$, and is largely facilitated by rewriting (2.7d,e) in the form

$$\partial_t\bar{\mathbf{u}}_i + \bar{\mu}_i\mathbf{u}_i^\sigma + h_i\hat{\mathbf{z}}\times(\bar{q}_i\bar{\mathbf{u}}_i + \tfrac{1}{3}q_i^\sigma\mathbf{u}_i^\sigma) + \boldsymbol{\nabla}\bar{b}_i = \bar{\mathbf{R}}_i, \tag{3.5a}$$

$$\partial_t\mathbf{u}_i^\sigma + h_i\hat{\mathbf{z}}\times(q_i^\sigma\bar{\mathbf{u}}_i + \bar{q}_i\mathbf{u}_i^\sigma) + \boldsymbol{\nabla}b_i^\sigma = \mathbf{R}_i^\sigma. \tag{3.5b}$$

Here,

$$\bar{\mu}_i := \tfrac{1}{3}h_i^{-1}\nabla\cdot h_i\mathbf{u}_i^\sigma \tag{3.6}$$

is the vertical average of the ith σ-vertical velocity;

$$\bar{q}_i := h_i^{-1}\left(f + \boldsymbol{\nabla}\cdot\bar{\mathbf{u}}_i\times\hat{\mathbf{z}}\right), \quad q_i^\sigma := h_i^{-1}\boldsymbol{\nabla}\cdot\mathbf{u}_i^\sigma\times\hat{\mathbf{z}} \tag{3.7}$$

are the mean and σ components of the ith-layer σ-potential vorticity, which are not Lagrangian constants of (2.7); and

$$\bar{\mathbf{R}}_i := \tilde{h}_{i-1}\boldsymbol{\nabla}\bar{\vartheta}_i + \tfrac{1}{2}h_i\boldsymbol{\nabla}(\bar{\vartheta}_i - \tfrac{1}{3}\vartheta_i^\sigma), \tag{3.8a}$$

$$\mathbf{R}_i^\sigma := (\tilde{h}_{i-1} + \tfrac{1}{2}h_i)\boldsymbol{\nabla}\vartheta_i^\sigma - \tfrac{1}{2}h_i\boldsymbol{\nabla}\bar{\vartheta}_i, \tag{3.8b}$$

which are rotational forces that arise as a consequence of the buoyancy inhomogeneities within each layer ($\boldsymbol{\nabla}\bar{\vartheta}_i \neq \mathbf{0} \neq \boldsymbol{\nabla}\vartheta_i^\sigma$).

In turn, the local conservation law for the sum of the zonal momenta within each layer is given by

$$\partial_t\sum_j M_j + \boldsymbol{\nabla}\cdot\sum_j \mathbf{F}_j^M + \partial_x h_0\sum_j h_j\bar{\vartheta}_j = 0, \tag{3.9a}$$

where

$$\mathbf{F}_i^M := M_i\bar{\mathbf{u}}_i + \tfrac{1}{3}h_i u_i^\sigma\mathbf{u}_i^\sigma + \tfrac{1}{2}\gamma h_i^2(\bar{\vartheta}_i - \tfrac{1}{3}\vartheta_i^\sigma)\hat{\mathbf{x}} + \gamma h_{i+1}\bar{\vartheta}_{i+1}\sum_{j=1}^{i-1}h_j\hat{\mathbf{x}} \tag{3.9b}$$

with u_i denoting the zonal component of $\mathbf{u}_i$ and $\hat{\mathbf{x}}$ the unit vector in the same direction†. The above result follows upon multiplying by γh_i the zonal component of (2.7d),

$$\partial_t\bar{u}_i + \bar{\mathbf{u}}_i\cdot\boldsymbol{\nabla}\bar{u}_i + \tfrac{1}{3}h_i^{-1}\boldsymbol{\nabla}\cdot h_i u_i^\sigma\mathbf{u}_i^\sigma - (f + \tau\bar{u}_i)\,\bar{v}_i + \gamma^{-1}\overline{\partial_x p}_i = 0, \tag{3.10}$$

and realizing that $\sum_j h_j\bar{\vartheta}_j\partial_x(\tilde{h}_{j-1} - h_0) + \sum_j h_j\partial_x\sum_{k=j+1}^n h_k\bar{\vartheta}_k \equiv \partial_x(\sum_j h_{j+1}\bar{\vartheta}_{j+1}\sum_{k=1}^{j-1}h_k)$. At this point it is crucial to specify whether the geometry is flat or spherical. On the sphere, $\boldsymbol{\nabla}a = \left(\gamma^{-1}\partial_x a, \partial_y a\right)$, for any scalar $a(\mathbf{x})$, and $\boldsymbol{\nabla}\cdot\mathbf{a} = \gamma^{-1}[\partial_x a + \partial_y(\gamma b)]$, for any vector $\mathbf{a} = (a, b)$, where $x = (\lambda - \lambda_0)\cos\theta\,R$ and $y = (\theta - \theta_0)R$ are, respectively, rescaled geographic longitude and latitude on the surface of the Earth whose mean radius is R; and $\gamma = \cos\theta_0\cos\theta$ and $\tau = R^{-1}\tan\theta \equiv -\gamma^{-1}\mathrm{d}\gamma/\mathrm{d}y$ are coefficients that characterize the geometry of the space (the arclength element square and area element are $\mathrm{d}\mathbf{x}^2 = \gamma^2\mathrm{d}x^2 + \mathrm{d}y^2$ and $\mathrm{d}^2\mathbf{x} = \gamma\mathrm{d}x\mathrm{d}y$, respectively). The ith zonal momentum (angular momentum around the Earth's axis) is then given by

$$M_i = h_i[\gamma\bar{u}_i - \Omega R(\cos\vartheta_0 - \gamma\cos\vartheta)], \tag{3.11}$$

where Ω is the Earth's angular rotation rate. In the classical β plane, $\gamma = 1$ and $\tau = 0$ so that all the operators are Cartesian and $M_i = h_i(\bar{u}_i - f_0 y - \tfrac{1}{2}\beta y^2)$. However, the geometry in a consistent β plane cannot be Cartesian; instead $\gamma = 1 - \tau_0 y$, $\tau = \tau_0/\gamma$, and $M_i = h_i[\gamma\bar{u}_i - f_0 y - \tfrac{1}{2}\beta(1 - R^2\tau_0^2)y^2]$ (Ripa 1997). Conservation of the total zonal momentum (sum over all layers) in a closed domain requires in addition, in all cases, that both the topography and coasts to be zonally symmetric.

† A term $-\tfrac{1}{6}\partial_x(h\vartheta_\sigma)$ is missing on the right hand side of (4.6) in R95.

3.2. *Kelvin circulation theorem(s)*

Letting $C_t(\bar{\mathbf{u}}_i)$ be a material curve that moves in the ith layer with the vertically averaged velocity $\bar{\mathbf{u}}_i$. Then taking into account (2.7c), from (**??**) it follows that

$$\frac{\mathrm{d}}{\mathrm{d}t}\oint_{C_t(\bar{\mathbf{u}}_i)} \mathrm{d}\mathbf{x}\cdot(\bar{\mathbf{u}}_i+\mathbf{u}_f) = \oint_{C_t(\bar{\mathbf{u}}_i)} \mathrm{d}\mathbf{x}\cdot(\bar{\mathbf{R}}_i + \tfrac{1}{3}h_i q_i^\sigma \mathbf{u}_i^\sigma \times \hat{\mathbf{z}} + \bar{\mu}_i \mathbf{u}_i^\sigma), \tag{3.12a}$$

$$\frac{\mathrm{d}}{\mathrm{d}t}\oint_{C_t(\bar{\mathbf{u}}_i)} \mathrm{d}\mathbf{x}\cdot\mathbf{u}_i^\sigma = \oint_{C_t(\bar{\mathbf{u}}_i)} \mathrm{d}\mathbf{x}\cdot(\mathbf{R}_i^\sigma + h_i\bar{q}_i\mathbf{u}_i^\sigma\times\hat{\mathbf{z}}), \tag{3.12b}$$

where $\boldsymbol{\nabla}\cdot\mathbf{u}_f\times\hat{\mathbf{z}} := f$. These are the Kelvin circulation theorem(s) for the multilayer model of this paper. The situation is different than in the fully three-dimensional model for which $\oint \mathrm{d}\mathbf{x}\cdot(\mathbf{v}|_\rho+\mathbf{u}_f)$, where $\mathbf{v}|_\rho$ is the (three-dimensional) velocity on a given isopycnal surface, is conserved. In the present case, $C_t(\bar{\mathbf{u}}_i)$ cannot remain on an isopycnal surface, which moves with $\mathbf{u}|_\rho$ at all times. If instead of $C_t(\bar{\mathbf{u}}_i)$ a rigid boundary were considered on which $\hat{\mathbf{n}}\times\boldsymbol{\nabla}\bar{\vartheta}_i \equiv \mathbf{0} \equiv \hat{\mathbf{n}}\times\boldsymbol{\nabla}\vartheta_i^\sigma$, where $\hat{\mathbf{n}}$ is the outer normal to the boundary, then the circulation of $\mathbf{u}_i^\sigma$ along that boundary would be preserved. Even though preservation of such a boundary condition is guaranteed by the dynamics, it is too restrictive to be expected. In the slab model, however, $\hat{\mathbf{n}}\times\boldsymbol{\nabla}\bar{\vartheta}_i \equiv \mathbf{0}$ on a rigid boundary, which is preserved by the dynamics, is necessary for the circulation along that boundary to be an (explicit) integral of motion, and for the Hamiltonian structure of the model not to be spoiled.

3.3. *Hamiltonian structure*

The (inviscid unforced) fully three-dimensional primitive equations model, just as the Euler equations of fluid mechanics, possesses what is called in geometric mechanics a "generalized or singular Hamiltonian structure." A good sign of the validity of any approximate model derived from it is the preservation of such a structure. This topic is treated here; readers not interested in geometric mechanics may safely skip this section.

Upon grouping $\boldsymbol{\varphi} = (\bar{\vartheta}_1, \vartheta_1^\sigma, h_1, \bar{\mathbf{u}}_1, \mathbf{u}_1^\sigma, \cdots, \bar{\vartheta}_n, \vartheta_n^\sigma, h_n, \bar{\mathbf{u}}_n, \mathbf{u}_n^\sigma)$ and defining $\mathcal{H}[\boldsymbol{\varphi}] := \sum_j \int_D \mathrm{d}^2\mathbf{x}\, E_j$, where the model equations (2.7) can be cast in the form

$$\partial_t\boldsymbol{\varphi} = \{\boldsymbol{\varphi}, \mathcal{H}\}. \tag{3.13}$$

Here, $\{\mathcal{A},\mathcal{B}\} := \int_D \mathrm{d}^2\mathbf{x}\,(\delta\mathcal{A}/\delta\boldsymbol{\varphi})\mathsf{J}(\delta\mathcal{B}/\delta\boldsymbol{\varphi})$ for any admissible functionals $\mathcal{A}[\boldsymbol{\varphi}]$ and $\mathcal{B}[\boldsymbol{\varphi}]$, where J is a skew-adjoint 7×7 block-diagonal matrix operator $\mathsf{J} = \bigoplus_j \mathsf{J}^1_{(j)} + \mathsf{J}^2_{(j)}$, with

$$\mathsf{J}^1_{(i)} := -\begin{pmatrix} 0 & 0 & 0 & 0 & 0 \\ 0 & 0 & 0 & 0 & 0 \\ 0 & 0 & 0 & \boldsymbol{\nabla}\cdot & 0 \\ 0 & 0 & \boldsymbol{\nabla} & \bar{q}_i\mathbf{z}\times & q_i^\sigma\mathbf{z}\times \\ 0 & 0 & 0 & q_i^\sigma\mathbf{z}\times & 3\bar{q}_i\mathbf{z}\times \end{pmatrix}, \tag{3.14a}$$

$$\mathsf{J}^2_{(i)} := -\begin{pmatrix} 0 & 0 & 0 & h_i^{-1}\boldsymbol{\nabla}\bar{\vartheta}_i\cdot & h_i^{-1}\boldsymbol{\nabla}\cdot\vartheta_i^\sigma \\ 0 & 0 & 0 & h_i^{-1}\boldsymbol{\nabla}\vartheta_i^\sigma\cdot & 3h_i^{-1}\boldsymbol{\nabla}\bar{\vartheta}_i\cdot \\ 0 & 0 & 0 & 0 & 0 \\ -h_i^{-1}\boldsymbol{\nabla}\bar{\vartheta}_i & -h_i^{-1}\boldsymbol{\nabla}\vartheta_i^\sigma & 0 & 0 & h_i^{-1}\mathbf{u}_i^\sigma\boldsymbol{\nabla}\cdot \\ \vartheta_i^\sigma\boldsymbol{\nabla}(h_i^{-1} & -3h_i^{-1}\boldsymbol{\nabla}\bar{\vartheta}_i & 0 & \boldsymbol{\nabla}(h_i^{-1}\mathbf{u}_i^\sigma\cdot & 0 \end{pmatrix}. \tag{3.14b}$$

Operators (3.14) are the same ones given by R95 for the one-layer model but particularized for ith layer. Thus an admissible functional $\mathcal{A}[\boldsymbol{\varphi}]$ must be such that $(\delta\mathcal{A}/\delta\bar{\mathbf{u}}_i)\cdot\hat{\mathbf{n}} = 0 =$

$(\delta\mathcal{A}/\delta\mathbf{u}_i^\sigma)\cdot\hat{\mathbf{n}}$ on ∂D. The functional derivatives of $\mathcal{H}$ are given by

$$\frac{\delta\mathcal{H}}{\delta\bar{\vartheta}_i} = h_i(\tilde{h}_{i-1} + \tfrac{1}{2}h_i),\ \frac{\delta\mathcal{H}}{\delta\vartheta_i^\sigma} = -\frac{h_i^2}{6},\ \frac{\delta\mathcal{H}}{\delta h_i} = h_i\bar{b}_i,\ \frac{\delta\mathcal{H}}{\delta\bar{\mathbf{u}}_i} = h_i\bar{\mathbf{u}}_i,\ \frac{\delta\mathcal{H}}{\delta\mathbf{u}_i^\sigma} = \frac{h_i\mathbf{u}_i^\sigma}{3}. \tag{3.15}$$

That system (2.7) can be put in the form (3.13) suggests that the layered model of this paper posses a singular Hamiltonian structure on the phase space given by the Cartesian product of the n manifolds whose coordinates are the 7 layer variables. The functional $\mathcal{H}$ and the operator $\{\cdot,\cdot\}$ being the Hamiltonian and Poisson bracket, respectively. (Proof of the Jacobi identity satisfied by the Poisson bracket—not given in R95—will be published elsewhere.) This conveys important properties like the direct linking of the conservation laws for energy, $\mathcal{H}$, and zonal momentum, $\mathcal{M}$, with symmetries via Noether's theorem (e.g. Shepherd 1990); notice that $\mathcal{H}$ and $-\mathcal{M}$ are the generators of t- and x-translations because of (3.13) and $\partial_x\boldsymbol{\varphi} = \{\mathcal{M},\boldsymbol{\varphi}\}$, respectively. In this framework the ith layer integrals of volume, $\mathcal{C}_i^0$, mass, $\mathcal{C}_i^1$, and buoyancy variance, $\mathcal{C}_i^2$, are invariant Casimirs, which satisfy $\{\mathcal{C}_i^j,\mathcal{F}\}\equiv 0\ \forall\mathcal{F}[\boldsymbol{\varphi}]$ and thus are not related to (explicit) symmetries; notice that $\mathcal{C}_i^j$ does not generate any transformation since $\{\boldsymbol{\varphi},\mathcal{C}_i^j\}\equiv 0$.

The existence of a Lie–Poisson Hamiltonian structure, which would imply an analogous Euler–Poincaré structure, has not been established for the present model. The Euler–Poincaré structure is based on a Lagrangian functional and Hamilton's principle, rather than a Hamiltonian functional and a Poisson bracket (Holm *et al.* 2002). The use of Hamilton's principle, in particular, has been shown very practical in the derivation of constrained dynamics (e.g. Salmon 1983; Holm 1996; Beron-Vera 2003) and approximate dynamics (Holm *et al.* 2002). An interesting research avenue is the exploration of whether approximations directly made in the fully-three dimensional Lagrangian can lead to the approximate model of the present paper. The study of these topics are reserved for the future.

3.4. *Arnold stability*

In R95 it was shown that for one layer a state of rest (or a steady state with at most a uniform zonal current) can be shown to be formally stable using Arnold's (1965, 1966) method if and only if (2.6) is satisfied, i.e. if and only if the buoyancy is everywhere positive and increases (resp., decreases) with depth within a layer with the rigid bottom (resp., rigid lid). Arnold's method for proving the stability of steady solution of a system consists in searching for conditions that guarantee the sign-definiteness of a general invariant which is quadratic to the lowest-order in the deviation from that state; the resulting conditions being only sufficient (e.g. Holm *et al.* 1985; McIntyre & Shepherd 1987). In the present model, however, Arnold's method fails to provide stability conditions even for a state of rest and with no topography ($h_0\equiv 0$). The lowest-order contribution to that quadratic invariant, which can be called a "free energy" because it corresponds to a state of rest,

$$\begin{aligned}\mathcal{E} := \tfrac{1}{2}\int_j & H_j(\delta\bar{\mathbf{u}}_j)^2 + \tfrac{1}{3}H_j(\delta\mathbf{u}_j^\sigma)^2 + (g_j - \tfrac{1}{2}N_j^2H_j)(\delta h_j)^2 \\ & + N_j^{-2}H_j(\delta\bar{\vartheta}_j + \tfrac{1}{2}N_j^2\delta h_j)^2 + \tfrac{1}{3}N_j^{-2}H_j(\delta\vartheta_j^\sigma - \tfrac{1}{2}N_j^2\delta h_j)^2 \\ & + (g_j\delta h_j + H_j\delta\bar{\vartheta}_j)\delta\tilde{h}_{j-1},\end{aligned} \tag{3.16}$$

cannot be proved sign-definite. Here,

$$\int_j (\cdot) := \sum_j \int_{D_j} \mathrm{d}^2\mathbf{x}\,(\cdot)\,, \tag{3.17}$$

and H_i, g_i and N_i, which are the ith-layer unperturbed depth, vertically averaged buoyancy, and Brunt–Väisälä frequency, respectively. Similarly, a state of rest in the multilayer slab model cannot be proved formally stable using Arnold's method. Surprisingly, it is possible to prove the stability of a steady state with a uniform zonal current in that model. But the condition of stability is not one of "static" stability like (2.6) as in the one-layer version of Ripa's model. Contrarily, it is one of "baroclinic" stability since a uniform current in the multilayer slab model has an implicit vertical shear through the thermal-wind balance. These results can all be inferred from Ripa (1993) and Ripa (1996).

It is worthwhile to mention, however, that there is at least a system, which has one Ripa-like layer and $n-1$ homogeneous layers, for which a state of rest can be proved formally stable. For instance, assuming the uppermost layer to be Ripa-like, the corresponding free energy takes the form

$$\begin{aligned}\mathcal{E} := \tfrac{1}{2}\int_j & H_j(\delta\bar{\mathbf{u}}_j)^2 + \tfrac{1}{3}H_\alpha(\delta\mathbf{u}^\sigma_\alpha)^2 \\ &+\tfrac{1}{2}N_\alpha^{-2}H_\alpha(\delta\bar{\vartheta}_\alpha + \tfrac{1}{2}N_\alpha^2\delta h_\alpha)^2 + \tfrac{1}{3}N_\alpha^{-2}H_\alpha(\delta\vartheta^\sigma_\alpha - \tfrac{1}{2}N_\alpha^2\delta h_\alpha)^2 \\ &+(g_j - g_{j+1})(\delta\tilde{h}_j)^2 - \tfrac{1}{2}N_\alpha^2 H_\alpha(\delta h_\alpha)^2, \end{aligned} \tag{3.18}$$

where $\alpha := n$ (resp., $\alpha := 1$) for the rigid-bottom (resp., rigid-lid) configuration, and H_i, g_i, and N_i are all constants. The above free energy is positive-definite if and only if (2.6) if fulfilled. [The homogeneous layers model has an infinite set of invariants which are given by $\int_j h_j F(\bar{q}_j)\ \forall F(\cdot)$; these include the volume integral, which is the only one needed to obtain the above result.] When all layers are homogeneous the same result is obtained. When one slab layer is included, however, the free energy cannot be shown of one sign.

The fact that it is not possible to prove formal stability for a steady state in the multilayer model of this paper does not mean that state is unstable; it simply means that Arnold's method is not useful to prove it. One reason for the failure of Arnold's method is the lack of vorticity-related invariants.

3.5. *Waves and instabilities*

In R95 it was shown that a model with one layer supports two vertical normal modes. The present n-layer model can support $3n-1$ in account for the extra $n-1$ baroclinic modes contributed by the n layers. A model with n homogeneous or slab layers only supports $2n$ vertical normal modes. Figure 3 shows, in particular, the phase speed of long gravity waves (c) for the barotropic and first baroclinic mode as a function of the stratification in the reference state, as predicted by the (exact) fully three-dimensional model,

$$\frac{N_\mathrm{r}H_\mathrm{r}}{2c}\tan\frac{N_\mathrm{r}H_\mathrm{r}}{c} = \frac{S}{1-S} \tag{3.19}$$

(cf. e.g. Gill 1982), and as predicted by the present model with one and two layers, and also by a model with two homogeneous layers. Here,

$$S := \tfrac{1}{2}N_\mathrm{r}^2 H_\mathrm{r}/g_\mathrm{r} \tag{3.20}$$

is a nondimensional measure of the stratification within the active layer, where H_r, g_r, and N_r denote the constant layer thickness, vertically averaged buoyancy, and Brunt–Väisälä frequency, respectively, in the motionless reference state (R95, Beron-Vera & Ripa, 1997). The reference state has a flat bottom/lid ($h_0 \equiv 0$) and a single, continuously stratified active layer with linear vertical stratification. The buoyancy varies from $g_\mathrm{r}(1\mp S)$, at the

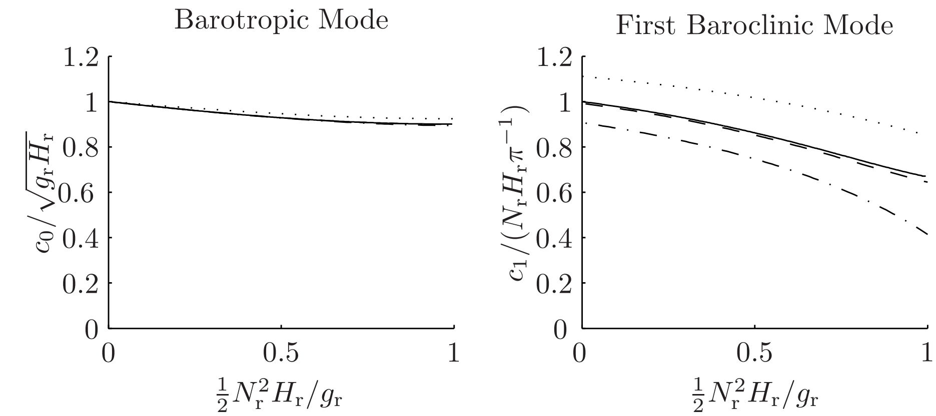

FIGURE 3. Phase speed of a long gravity wave for the barotropic (c_0) and first baroclinic (c_1) modes as a function of the stratification of the reference state, as predicted by the fully-three dimensional model (solid lines), a one- (dot-dashed lines) and two-layer (dashed) versions of the present multilayer model, and a two-homogenous-layer model (dotted lines). In this figure, H_r, g_r, and N_r are the constant reference depth, mean buoyancy, and Brunt–Väisälä frequency, respectively.

top of the active layer, to $g_\mathrm{r}(1 \pm S)$, at the base of the active layer. As a consequence of condition (2.6), $0 < S < 1$. Notice that this condition does not limit the size of the density gradient within the active layer: the buoyancy change within the layer, $N_\mathrm{r}^2 H_\mathrm{r} = 2Sg_\mathrm{r}$, can be made as large as desired while keeping fixed the buoyancy at the interface with the inert layer $g_\mathrm{r}(1 - S)$. The present layer model reference state parameters are chosen as

$$H_i = \frac{H_\mathrm{r}}{n}, \quad g_i = g_r \left[1 + \left(1 - \frac{2i-1}{n}\right) S\right], \quad N_i = \frac{g_\mathrm{r} S}{H_\mathrm{r}}, \tag{3.21}$$

with $n = 1, 2$. The ith layer reference depth H_i and layer buoyancy g_i for the model with two homogeneous layers are chosen as in (3.21). [Other choices for the two-homogeneous-layer model parameters, which can be made to match the three-dimensional model's phase speed at a fixed value of S, are of course possible (e.g. Olascoaga & Ripa 1999).] For this model it is (cf. e.g. Gill 1982)

$$c^2 = g_\mathrm{r} H_\mathrm{r} \frac{S - S^2/2}{2 \pm 2\sqrt{1 - S + S^2/2}}. \tag{3.22}$$

The long-gravity-wave phase speeds of the model of this paper are computed numerically by setting $f \equiv 0$ in (2.7) and considering infinitesimal normal-mode perturbations to (3.21). The left-hand-side panel of figure 3 shows that a one-layer version of the model generalized here (dot-dashed line) is enough to represent the exact (solid line) barotropic mode phase speed (c_0) for all values of the stratification parameter S (R95). The result from a two-layer version (dashed line) cannot be distinguished from the one-layer version and exact results in this plot. The two-homogeneous-layer model (dotted line) gives the exact phase speed at very weak stratification ($S \to 0$) but overestimates it somewhat as the stratification increases. The most striking differences appear in the representation of the baroclinic mode phase speed. The right-hand-side panel of figure 3 shows that the one-layer version of the model of this paper provides only a fair representation of the phase speed of the gravest baroclinic mode (c_1). The two-layer version, instead, provides an excellent approximation for any size of S. The two-homogeneous-layer model phase speed, in turn, overestimates the exact model phase speed for all S (the absolute value of difference being of the same order as that produced by the one-layer version of the present model). The reason for the improved performance of the two-layer version of present model compared to the one-layer version and the two-homogeneous-layer model is that with one linear function in each layer is possible to better represent the exact vertical structure eigenfunctions than with only one linear function and one number per layer, respectively. A considerable amount of "physics" is gained by adding to the velocity and buoyancy fields a vertical shear within each layer following the simple recipe proposed by R95. In Beron-Vera *et al.* (2003) we extend and complete the above calculation by considering more complicated reference vertical stratifications and computing the vertical structure eigenfunctions. We also show that the present model supports the usual midlatitude and equatorial gravity and vortical waves (Poincaré, Kelvin, Rossby, Yanai, etc.) in each of the vertical normal modes.

Let me close this section by making some remarks on baroclinic instability results. To study baroclinic instability in the upper ocean, Beron-Vera & Ripa (1997) considered a reduced-gravity approximation. In that work it was shown that a reduced-gravity one-layer version of Ripa's model gives, in the limit of weak internal stratification and sufficiently strong velocity's vertical shear, the exact solution for normal-mode perturbations whose scales are of the order of the external (equivalent barotropic) deformation radius of the system. For perturbations of the order of the internal (first baroclinic) deformation radius, i.e. the classical Eady "waves" (cf. e.g. Pedlosky 1987), the model resulted less successful as the exact eigensolutions have an exponential trapping behavior which can be only poorly represented if the velocity and buoyancy vertical profiles are restricted to a linear function of depth. The very important dynamical aspect of the presence of a high-wavenumber cutoff of instability was nonetheless captured by the one-layer model, though overestimated in about 40 %. By virtue of the above results, I expect this overestimation to be substantially reduced if two active layers are considered. This is investigated in Beron-Vera *et al.* (2003) where we further test the present model performance in upper-ocean baroclinic instability including ageostrophic effects. The latter is done by relaxing the rigid bottom boundary constraint in the classical Stone (1966) model.

3.6. *Forcing*

In R95 forcing (wind stress, interfacial drag, and buoyancy/heat input) was introduced in the one-layer version of the present multilayer model equations in a way that was compatible with the conservation laws of energy, momentum, and mass/heat content. The same approach is adopted here to include, in addition, freshwater fluxes through the surface in accordance with the conservation law of salt content. The possibility for the exchange of fluid across the other interfaces is also considered.

Let $\boldsymbol{\tau}(\mathbf{x}, t)$ be a wind stress acting at the surface of the ocean ($\rho_{n+1} \equiv 0$ must be the setting in the rigid-bottom configuration and typically $h_0 \equiv 0$ in the rigid-lid one). Assume further that there is a friction force acting at the interface between contiguous layers. Introduction of these forces in Newton's equations (2.7d,e) in the form

$$\partial_t \bar{\mathbf{u}}_i + \cdots = \delta_{i\alpha} \boldsymbol{\tau}/h_\alpha - r_i(\bar{\mathbf{u}}_i \pm \mathbf{u}_i^\sigma), \tag{3.23a}$$

$$\partial_t \mathbf{u}_i^\sigma + \cdots = \mp 3\delta_{i\alpha} \boldsymbol{\tau}/h_\alpha + 3r_i(\bar{\mathbf{u}}_i \pm \mathbf{u}_i^\sigma), \tag{3.23b}$$

implies that the work done by the wind stress is proportional to the velocity at the top of the uppermost layer, $\bar{\mathbf{u}}_\alpha \mp \mathbf{u}_\alpha^\sigma$, and that one done by the friction force in the ith layer is proportional to the velocity at the base of that layer, $\bar{\mathbf{u}}_i \pm \mathbf{u}_i^\sigma$. Namely

$$\partial_t \sum_j E_j + \cdots = \boldsymbol{\tau} \cdot (\bar{\mathbf{u}}_\alpha \mp \mathbf{u}_\alpha^\sigma) - \sum_j r_j h_j (\bar{\mathbf{u}}_j \pm \mathbf{u}_j^\sigma)^2, \tag{3.24a}$$

$$\partial_t \sum_j M_j + \cdots = \boldsymbol{\tau} \cdot \hat{\mathbf{x}} - \sum_j r_j h_j (\bar{\mathbf{u}}_j \pm \mathbf{u}_j^\sigma) \cdot \hat{\mathbf{x}}. \tag{3.24b}$$

In the above equations, δ_{ij} is the Kroenecker delta and r_i is a friction coefficient that can be taken as a constant or as some function of h_i and $|\bar{\mathbf{u}}_i \pm \mathbf{u}_i^\sigma|$. [Recall that $\alpha := n$ (resp., $\alpha := 1$) for the rigid-bottom (resp., rigid-lid) configuration.]

Let now $\Gamma(\mathbf{x}, t)$ be a buoyancy input through the surface and introduce it in the buoyancy equations (2.7a,b) in the form

$$\partial_t \bar{\vartheta}_i + \cdots = \delta_{i\alpha} \Gamma / h_\alpha, \tag{3.25a}$$

$$\partial_t \vartheta_i^\sigma + \cdots = \eta \delta_{i\alpha} \Gamma / h_\alpha, \tag{3.25b}$$

where η is any constant. Consider, in addition, the possibility of fluid crossing the interface between consecutive layers; then the volume conservation equation (2.7c) can be rewritten as

$$\partial_t h_i + \cdots = w_i^{\mathrm{b}} - w_i^{\mathrm{t}}. \tag{3.25c}$$

Here, the quantities $w_i^{\mathrm{t}}(\mathbf{x}, t)$ and $w_i^{\mathrm{b}}(\mathbf{x}, t)$ are volume fluxes per unit area through the top and base of the ith layer, respectively. The set (3.25), for any value of η, is compatible with the mass conservation equation

$$\partial_t (h_i \bar{\vartheta}_i) + \cdots = \delta_{i\alpha} \Gamma + \bar{\vartheta}_i (w_i^{\mathrm{b}} - w_i^{\mathrm{t}}). \tag{3.26}$$

At the surface $w_\alpha^{\mathrm{t}}(\mathbf{x}, t) = P(\mathbf{x}, t) - E(\mathbf{x}, t)$, which represents the imbalance of precipitation minus evaporation; away from the surface some parametrization must be adopted. In models with slab layers it is commonly set (e.g. McCreary *et al.* 1991)

$$w_i^{\mathrm{b}} - w_i^{\mathrm{t}} = \begin{cases} (-1)^{i+1} \dfrac{(h_{i-1} - H_{i-1}^{\mathrm{e}})^2}{H_{i-1}^{\mathrm{e}} t_i^{\mathrm{e}}} & \text{if } h_{i-i} \leqslant H_{i-1}^{\mathrm{e}}, \\ 0 & \text{if } h_{i-1} > H_{i-1}^{\mathrm{e}}. \end{cases} \tag{3.27}$$

Here, H_i^{e} and t_i^{e} are constants that with units of length and time, respectively, that characterize the "entrainment" process. In the present case, an algorithm may be design such that condition (2.6) is fulfilled at all times. This would allow for the inclusion of mixing processes in a novel and rather physical way. On the other hand, mixing events are known to occur in localized regions of the ocean, which can be represented by regions where $\bar{\vartheta}_{i+1} + \vartheta_{i+1}^\sigma < \bar{\vartheta}_i - \vartheta_i^\sigma$ instantaneously. This subject deserves to be studied in detail.

Let finally assume a linear state equation, i.e. $\vartheta_i = g\alpha_T (T_i - T_{n+1}) - g\alpha_S (S_i - S_{n+1})$. Here, α_T and α_S are the thermal expansion and salt contraction coefficients, respectively; $T_i(\mathbf{x}, \sigma, t) = \bar{T}_i(\mathbf{x}, t) + \sigma T_i^\sigma(\mathbf{x}, t)$ and $S_i(\mathbf{x}, \sigma, t) = \bar{S}_i(\mathbf{x}, t) + \sigma S_i^\sigma(\mathbf{x}, t)$ are the ith layer temperature and salinity, respectively; and T_{n+1} and S_{n+1} are the inactive layer (constant) temperature and salinity, respectively. Let also write the buoyancy input as

$$\Gamma = g\alpha_T (\rho_{\mathrm{r}} C_p)^{-1} Q + g\alpha_S \bar{S}_\alpha (P - E). \tag{3.28}$$

Here, C_p is the specific heat at constant pressure and $Q(\mathbf{x}, t)$ is the heat input through the surface. Equation (3.26) can then be split into a heat and salt content conservation equations, namely

$$\partial_t(h_i\bar{T}_i) + \cdots = \delta_{i\alpha}(\rho_{\rm r}C_p)^{-1}Q + \bar{T}_i(w_i^{\rm b} - w_i^{\rm t}), \tag{3.29a}$$

$$\partial_t(h_i\bar{S}_i) + \cdots = \delta_{i\alpha}\bar{S}_\alpha(E-P) + \bar{S}_i(w_i^{\rm b} - w_i^{\rm t}). \tag{3.29b}$$

If fluid across the surface is allowed only, the choice (3.28) enforces, on one hand (e.g. Beron-Vera *et al.* 1999)

$$\frac{\rm d}{{\rm d}t}\int_j h_j\bar{S}_j \equiv 0, \tag{3.30a}$$

and, on the other Beron-Vera & Ripa (2000)

$$\frac{\rm d}{{\rm d}t}\langle T\rangle = V^{-1}\int_D {\rm d}^2\mathbf{x}\,(\rho_{\rm r}C_p)^{-1}Q + (\bar{T}_\alpha - \langle T\rangle)(P-E), \tag{3.30b}$$

where $V := \int_j h_j \equiv \int_D {\rm d}^2\mathbf{x}\ h$ is the total volume and $\langle T\rangle := V^{-1}\int_j h_j\bar{T}_j$ is the average temperature in V. Notice that (3.30b), unlike the equation satisfied by $\int_j h_j\bar{T}_j$, is independent of the choice of the origin of the temperature scale (cf. Warren 1999).

4. Concluding remarks

This paper describes a multilayer extension of Ripa's (1995) primitive equations one-layer ocean model with thermodynamics. Inside each layer the velocity and buoyancy fields can vary not only arbitrarily in the horizontal position and time, but also linearly with depth. In the absence of external forcing and dissipation, the model conserves volume, mass, buoyancy variance, energy, and zonal momentum for a zonally symmetric domains and topographies. Furthermore, as the fully three-dimensional primitive equations from which it is derived, the present model possesses a singular Hamiltonian structure. Unlike the multilayer slab models, i.e. those for which the velocity and buoyancy fields are depth-independent within each layer, the model generalized here is able to represent the thermal-wind balance explicitly at low frequency inside each layer. In this sense, the model of this paper has better "physics" than a model with slab-like layers. For the same number of layers, n, say, on the other hand, the model of this paper can sustain $2n-1$ more vertical normal modes as homogeneous layers models, which, in addition, are not able to incorporate thermodynamic processes. A model with only two layers has been shown here to provide an excellent representation of the exact first baroclinic mode phase speed. In this other sense, the present model has more "physics" than a model with homogeneous layers. The present generalization enriches Ripa's single-layer model by providing it enough flexibility to approach problems for which a single-layer structure is too idealized. Configurations with a small number of layers are particularly useful for the insight they provide into physical processes. Configurations with more layers can be used as the basis for an accurate numerical circulation model.

This paper has benefited from conversations with Josefina Olascoaga, Javier Zavala-Garay, Mohamed Iskandarani, Mike Brown, and Rigo García.

REFERENCES

Anderson, D. & McCreary, J. 1985*a* On the role of the indian ocean in a coupled ocean-atmosphere model of el niño and the southern oscillation. *J. Atmos. Sci.* **42**, 2439–2442.

Anderson, D. L. T. & McCreary, J. P. 1985*b* Slowly propagating disturbances in a coupled Ocean-Atmosphere model. *J. Atmos. Sci.* **42**, 615–629.

Arnold, V. 1965 Condition for nonlinear stationary plane curvilinear flows of an ideal fluid. *Dokl. Akad. Nauk. USSR* **162**, 975–978, engl. transl. *Sov. Math.* **6**: 773-777 (1965).

Arnold, V. 1966 On an apriori estimate in the theory of hydrodynamical stability. *Izv. Vyssh. Uchebn. Zaved Mat.* **54**, 3–5, engl. transl. *Am. Math. Soc. Transl. Series II* **79**: 267-269 (1969).

Balmaseda, M. A., Anderson, D. L. T. & Davey, M. K. 1994 ENSO prediction using a dynamical ocean model coupled to statistical atmospheres. *Tellus A* **46**, 497–511.

Beier, E. 1997 A numerical investigation of the annual variability in the Gulf of California. *J. Phys. Oceanogr.* **27**, 615–632.

Beier, E. & Ripa, P. 1999 Seasonal gyres in the northern Gulf of California. *J. Phys. Oceanogr.* **29**, 305–311.

Beron-Vera, F. J. 2003 Constrained-Hamiltonian shallow-water dynamics on the sphere. In *Nonlinear Processes in Geophysical Fluid Dynamics: A Tribute to the Scientific Work of Pedro Ripa* (ed. O. U. Velasco-Fuentes, J. Sheinbuam & J. Ochoa). Kluwer, in press (e-Print arXiv:physics/0307141).

Beron-Vera, F. J., Ochoa, J. & Ripa, P. 1999 A note on boundary conditions for salt and freshwater balances. *Ocean Modell.* **1**, 111–118.

Beron-Vera, F. J., Olascoaga, M. J. & Zavala-Garay, J. 2003 Waves and instabilities in a multiayer primitive equations model with variable velocity shear and stratification. *J. Phys. Oceanogr.*, to be submitted.

Beron-Vera, F. J. & Ripa, P. 1997 Free boundary effects on baroclinic instability. *J. Fluid Mech.* **352**, 245–264.

Beron-Vera, F. J. & Ripa, P. 2000 Three-dimensional aspects of the seasonal heat balance in the Gulf of California. *J. Geophys. Res.* **105**, 11,441–11,457.

Beron-Vera, F. J. & Ripa, P. 2002 Seasonal salinity balance in the Gulf of California. *J. Geophys. Res.* **107** (C8), 10.1029/2000JC000769.

Bleck, R., Rooth, C., Hu, D. & Smith, L. 1992 Salinity-driven thermocline transients in a wind- and thermohaline-forced isopycnic coordinate model of the north atlantic. *J. Phys. Oceanogr.* **22**, 1486–1505.

Dronkers, J. 1969 Tidal computations in rivers, coastal areas and seas. *J. Hydrau. Div.* **95**, 44–77.

Eldevik, T. 2002 On frontal dynamics in two model oceans. *J. Phys. Oceanogr.* **32**, 2,915–2,925.

Fukamachi, Y., McCreary, J. P. & Proehl, J. A. 1995 Instability of density fronts in layer and continuously stratified models. *J. Geophys. Res.* **100**, 2559–2577.

Gill, A. E. 1982 *Atmosphere-Ocean Dynamics*. Academic.

Holm, D. D. 1996 Hamiltonian balance equations. *Physica D* **98**, 379–414.

Holm, D. D., Marsden, J. E., Ratiu, T. & Weinstein, A. 1985 Nonlinear stability of fluid and plasma equilibria. *Phys. Rep.* **123**, 1–116.

Holm, D. D., Marsden, J. E. & Ratiu, T. S. 2002 The Euler-Poincaré equations in geophysical fluid dynamics. In *Large-Scale Atmosphere-Ocean Dynamics II: Geometric Methods and Models* (ed. J. Norbury & I. Roulstone), pp. 251–299. Cambridge University.

Hood, R. R., Kohler, K. E., Jr., J. P. M. & Smith, S. L. 2003 A 4-dimensional validation of a coupled physical–biological model of the Arabian Sea. *Deep Sea Res.*, in press.

Lavoie, R. 1972 A mesoscale numerical model of lake-effect storms. *J. Atmos. Sci.* **29**, 1025 – 1040.

McCreary, J. P., Fukamachi, Y. & Kundu, P. 1991 A numerical investigation of jets and eddies near an eastern ocean boundary. *J. Geophys. Res.* **96**, 2515–2534.

McCreary, J. P., Han, W., Sahnkar, D. & Shetye, S. R. 1996*a* Dynamics of the East India coastal current 2. Numerical solutions. *J. Geophys. Res.* **101**, 13,993–14,010.

McCreary, J. P., Kohler, K. E., Hood, R. R. & Olson, D. B. 1996*b* A four-component ecosystem model of biological activity in the Arabian Sea. *Prog. Oceanog.* **37**, 193–240.

McCreary, J. P., Kohler, K. E., Hood, R. R., Smith, S., Fischer, A. S. & Weller, R. A. 2001 Influences of diurnal and intraseasonal forcing on mixed-layer and biological variability in the central arabian sea. *J. Geophys. Res.* **106**, 7139–7155.

McCreary, J. P. & Kundu, P. 1988 A numerical investigation of the Somali current during the southwest monsoon. *J. Mar. Res.* **46**, 25–58.

McCreary, J. P., Kundu, P. & Molinari, R. 1993 A numerical investigation of dynamics, thermodynamics and mixed-layer processes in the Indian Ocean. *Prog. Oceanog.* **31**, 181–244.

McCreary, J. P., Lee, H. & Enfield, D. 1989 The response of the coastal ocean to strong offshore winds: With application to circulations in the Gulfs of Tehuantepec and Papagayo. *J. Mar. Res.* **47**, 81–109.

McCreary, J. P. & Yu, Z. 1992 Equatorial dynamics in a $2\frac{1}{2}$-layer model. *Prog. Oceanogr.* **29**, 61–132.

McIntyre, M. & Shepherd, T. 1987 An exact local conservation theorem for finite-amplitude disturbances to non-parallel shear flows, with remarks on Hamiltonian structure and on Arnol'd's stability theorems. *J. Fluid Mech.* **181**, 527–565.

Olascoaga, M. J. & Ripa, P. 1999 Baroclinic instability in a two-layer model with a free boundary and β effect. *J. Geophys. Res.* **104**, 23,357–23,366.

Palacios-Hernández, E., Beier, E., Lavín, M. F. & Ripa, P. 2002 The effect of winter mixing on the circulation of the northern Gulf of California. *J. Phys. Oceanogr.* **32**, 705–728.

Pedlosky, J. 1987 *Geophysical Fluid Dynamics*. Second Edition, Springer.

Ripa, P. 1993 Conservation laws for primitive equations models with inhomogeneous layers. *Geophys. Astrophys. Fluid Dyn.* **70**, 85–111.

Ripa, P. 1995 On improving a one-layer ocean model with thermodynamics. *J. Fluid Mech.* **303**, 169–201.

Ripa, P. 1996 Linear waves in a one-layer ocean model with thermodynamics. *J. Geophys. Res. C* **101**, 1233–1245.

Ripa, P. 1997 Towards a physical explanation of the seasonal dynamics and thermodynamics of the Gulf of California. *J. Phys. Oceanogr.* **27**, 597–614.

Ripa, P. 1999 On the validity of layered models of ocean dynamics and thermodynamics with reduced vertical resolution. *Dyn. Atmos. Oceans* **29**, 1–40.

Ripa, P. 2001 To what extent are sea level variations due to the expansion or contraction of the water column? In *Proceedings of the 13th Conference on Atmospheric and Oceanic Fluid Dynamics*, pp. 1–4. American Meteorological Society.

Røed, L. P. 1997 Energy diagnostics in a $1\frac{1}{2}$-layer, nonisopycnic model. *J. Phys. Oceanogr.* **27**, 1,472–1,476.

Røed, L. P. & Shi, X. B. 1999 A numerical study of the dynamics and energetics of cool filaments, jets and eddies off the Iberian Peninsula. *J. Geophys. Res.* **104**, 29,817–29,841.

Salmon, R. 1983 Practical use of Hamilton's principle. *J. Fluid Mech.* **132**, 431–444.

Schopf, P. & Cane, M. 1983 On equatorial dynamics, mixed layer physics and sea surface temperature. *J. Phys. Oceanogr.* **13**, 917–935.

Scott, R. B. & Willmott, A. J. 2002 Steady-state frictional geostrophic circulation in a one-layer ocean model with thermodynamics. *Dyn. Atmos. Oce.* **35**, 389–419.

Shepherd, T. 1990 Symmetries, conservation laws, and Hamiltonian structure in geophysical fluid dynamics. *Adv. Geophys.* **32**, 287–338.

Stone, P. 1966 On non-geostrophic baroclinic stability. *J. Atmos. Sci.* **23**, 390–400.

Szoeke, R. A. d. & Richman, J. G. 1984 On wind-driven mixed layers with strong horizontal gradients - A theory with applications to coastal upwelling. *J. Phys. Oceanogr.* **14**, 364–377.

Warren, B. A. 1999 Approximating the energy transport across oceanic sections. *J. Geophys. Sci.* **104**, 7915–7919.

Young, W. 1994 The subinertial mixed layer approximation. *J. Phys. Oceanogr.* **24**, 1812–1826.

Young, W. & Chen, L. 1995 Baroclinic instability and thermohaline gradient alignment in the mixed layer. *J. Phys. Oceanogr.* **25**, 3172–3185.